



Evidence of a $J/\psi K_S^0$ structure in $B^0 \rightarrow J/\psi \phi K_S^0$ decays

LHCb collaboration

Abstract

An amplitude analysis of $B^0 \rightarrow J/\psi \phi K_S^0$ decays is performed using proton-proton collision data corresponding to an integrated luminosity of 9 fb^{-1} , collected with the LHCb detector at centre-of-mass energies of 7, 8 and 13 TeV. Evidence with a significance of 4.0 standard deviations of a structure in the $J/\psi K_S^0$ system, named $T_{\psi s1}^\theta(4000)^0$, is seen, with its mass and width measured to be $3991_{-10}^{+12} {}_{-17}^{+9} \text{ MeV}$ and $105_{-25}^{+29} {}_{-23}^{+17} \text{ MeV}$, respectively, where the first uncertainty is statistical and the second systematic. The $T_{\psi s1}^\theta(4000)^0$ state is likely to be the isospin partner of the $T_{\psi s1}^\theta(4000)^+$ state, previously observed in the $J/\psi K^+$ system of the $B^+ \rightarrow J/\psi \phi K^+$ decay. When isospin symmetry for the charged and neutral $T_{\psi s1}^\theta(4000)$ states, is assumed, the signal significance increases to 5.4 standard deviations.

Submitted to Phys. Rev. Lett.

Hadrons formed by more than three quarks, namely exotic hadrons, can have complex colour and flavour structures, and studies of their internal dynamics shed light on the non-perturbative behaviour of quantum chromodynamics at low energy. Since the discovery of the $\chi_{c1}(3872)$ state [1], several states compatible with a four or five quark composition have been observed [2], including the fully charmed tetraquark states [3–5] and the pentaquark states [6, 7]. In 2020, the BESIII collaboration reported the observation of the $T_{\psi_s}(3985)^+$ state in the $D_s^+\bar{D}^{*0}$ and $D_s^{*+}\bar{D}^0$ mass spectra [8].¹ Two similar states, $T_{\psi_{s1}}^\theta(4000)^+$ and $T_{\psi_{s1}}(4220)^+$, were observed in $B^+ \rightarrow J/\psi\phi K^+$ decays by the LHCb experiment [9].² With a minimum quark content of $c\bar{c}u\bar{s}$, these states are explicitly exotic. The observations of the $T_{\psi_{s1}}^\theta(4000)^+$, $T_{\psi_{s1}}(4220)^+$, and $T_{\psi_s}(3985)^+$ states have stimulated many theoretical studies to interpret their internal structures, such as hadronic molecules [11] or compact tetraquarks [12].

Searching for the isospin partners of the $T_{\psi_s}^+$ states, the $T_{\psi_s}^0$ states, provides another opportunity to better understand hidden-charm tetraquarks with strangeness. The quark contents for the $T_{\psi_s}^+$ and $T_{\psi_s}^0$ states are $c\bar{c}u\bar{s}$ and $c\bar{c}d\bar{s}$, respectively. Recently, the BESIII experiment reported evidence for the $T_{\psi_s}(3985)^0$ state ($c\bar{c}d\bar{s}$) in the $D_s^+D^{*-}$ and $D_s^{*+}D^-$ mass spectra [13]. The $B^0 \rightarrow J/\psi\phi K_S^0$ decay is an ideal candidate to search for such $T_{\psi_s}^0$ states. The quark level processes of the $B^0 \rightarrow J/\psi\phi K_S^0$ decay are similar to those of the $B^+ \rightarrow J/\psi\phi K^+$ decay, as shown in Fig. 1, and the two decays are related by isospin symmetry.

In this Letter, evidence of a $J/\psi K_S^0$ structure is reported from an amplitude analysis of $B^0 \rightarrow J/\psi\phi K_S^0$ decays. The analysis is based on proton-proton (pp) collision data, collected with the LHCb detector at centre-of-mass energies of 7 TeV, 8 TeV, and 13 TeV, corresponding to integrated luminosities of 1 fb^{-1} , 2 fb^{-1} , and 6 fb^{-1} , respectively.

The LHCb detector is a single-arm forward spectrometer covering the pseudorapidity range $2 < \eta < 5$, described in detail in Refs. [14, 15]. Simulated samples of the signal decays are used to estimate the effect of reconstruction and event selections. The samples are generated with PYTHIA [16], EVTGEN [17], and the GEANT4 toolkit [18] as described in Ref. [19].

For the $B^0 \rightarrow J/\psi\phi K_S^0$ decays, the J/ψ , ϕ , and K_S^0 candidates are reconstructed by

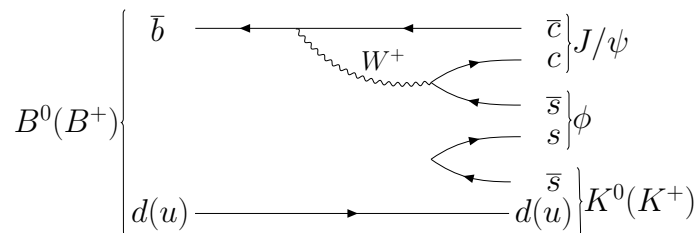


Figure 1: One of the Feynman diagrams contributing to $B^+ \rightarrow J/\psi\phi K^+$ or $B^0 \rightarrow J/\psi\phi K_S^0$ decays.

¹Charge conjugation is implied throughout the Letter unless specified otherwise.

²The new exotic hadron naming convention proposed by the LHCb collaboration [10] is applied throughout the Letter. The $T_{\psi_s}(3985)^+$, $T_{\psi_{s1}}^\theta(4000)^+$, and $T_{\psi_{s1}}(4220)^+$ states are named $Z_{cs}(3985)^+$, $Z_{cs}(4000)^+$, and $Z_{cs}(4220)^+$ in the original papers [8, 9], respectively. The superscript θ refers to 1/2 isospin and positive parity.

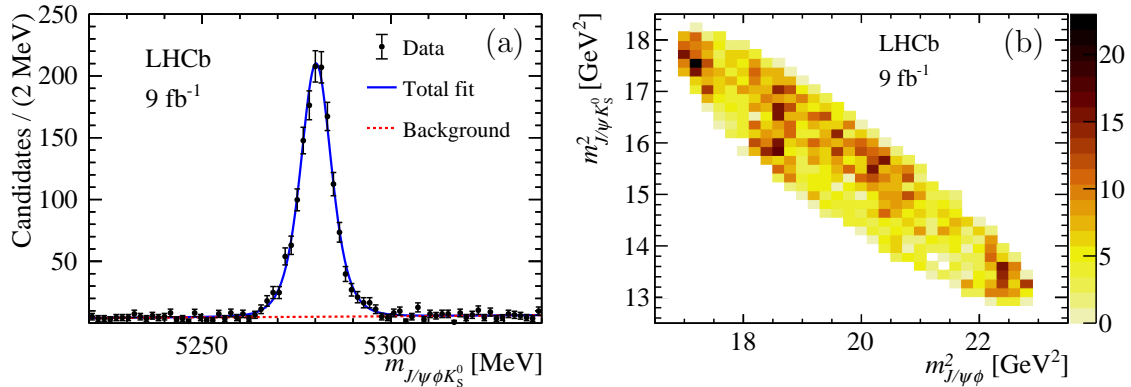


Figure 2: (a) Invariant-mass distribution of selected B^0 candidates and corresponding fit result. (b) The distribution of $m^2_{J/\psi K_S^0}$ versus $m^2_{J/\psi\phi}$ for candidates in the ± 15 MeV region around the known B^0 mass.

combining two oppositely charged muons, kaons, and pions, respectively, forming vertices detached from any primary vertex (PV). The B^0 candidate is reconstructed by combining the J/ψ , ϕ , and K_S^0 candidates and the resulting decay vertex must be of high quality. In order to improve the resolution of the mass of the B^0 candidates (referred to as $m_{J/\psi\phi K_S^0}$), a kinematic fit [20] is applied, with the J/ψ and K_S^0 masses constrained to their known values [2] and the B^0 candidates constrained to originate from their associated PVs. The associated PV is the one with smallest impact parameter χ^2 , defined as the difference in the vertex-fit χ^2 of a given PV with and without the particle under consideration.

The B^0 candidates are selected by a multivariate classifier based on a multilayer perceptron [21, 22]. The selection is similar to that used in Ref. [9], with an additional requirement on the significance of the flight distance of the K_S^0 from the B^0 decay vertex. Only candidates with the mass of the K^+K^- system within ± 15 MeV around the known ϕ mass [2] are kept.³ The multivariate classifier uses eleven variables related to the decay-chain topology, particle transverse momentum, vertex fit quality, and charged particle identification information. The selection criterion on the classifier response is chosen by maximising the figure of merit, $\mathcal{S}^2/(\mathcal{S} + \mathcal{B})^{3/2}$ [23], where \mathcal{S} and \mathcal{B} are the yields of signal and background in the signal region, respectively. The signal region in $m_{J/\psi\phi K_S^0}$ is defined to be ± 15 MeV around the known B^0 mass [2].

An extended maximum-likelihood fit is performed to the $m_{J/\psi\phi K_S^0}$ distribution of the selected candidates, as is shown in Fig. 2a. The B^0 signal is described by a Hypatia function [24] and the background is described by an exponential function. The B^0 yield is measured to be 1866 ± 47 in the signal region. The fraction of combinatorial background in the signal region is 6%. Roughly 4% of the B^0 yield corresponds to peaking-background $B^0 \rightarrow J/\psi K^+ K^- K_S^0$ decays without an intermediate ϕ meson (referred to as non- ϕ). The non- ϕ contribution is neglected in the default amplitude model and is considered as a source of systematic uncertainty. A further kinematic fit is performed to improve the momentum resolution of the final-state particles by constraining the measured B^0 mass to its known value. Figure. 2b shows the distribution of $m^2_{J/\psi K_S^0}$ versus $m^2_{J/\psi\phi}$ for candidates in the signal region.

³Natural units with $\hbar = c = 1$ are used throughout the Letter.

A simultaneous amplitude fit is performed to the $B^0 \rightarrow J/\psi\phi K_S^0$ and $B^+ \rightarrow J/\psi\phi K^+$ samples. The $B^+ \rightarrow J/\psi\phi K^+$ sample is the same as that used for the observation of the $T_{\psi s1}^\theta(4000)^+$ and $T_{\psi s1}(4220)^+$ states [9]. The likelihood for the B^0 decay is given by

$$\mathcal{L}(\vec{\omega}) = \prod_i \left[(1 - \beta) \mathcal{P}_{\text{sig}}(m_{\phi K_S^0}^i, \vec{\Omega}^i | \vec{\omega}) + \beta \mathcal{P}_{\text{bkg}}(m_{\phi K_S^0}^i, \vec{\Omega}^i) \right], \quad (1)$$

where the probability density functions (PDFs) for the signal and background components are given by $\mathcal{P}_{\text{sig}}(m_{\phi K_S^0}^i, \vec{\Omega}^i | \vec{\omega})$ and $\mathcal{P}_{\text{bkg}}(m_{\phi K_S^0}^i, \vec{\Omega}^i)$, respectively. The superscript i refers to the i -th candidate. The fraction of combinatorial background, β , is fixed to 6%. The likelihood of the B^+ decay is similar to Eq. 1 and is described in detail in Ref. [25]. The decay kinematics are described by a mass, chosen to be $m_{\phi K_S^0}$, and five angular variables $\vec{\Omega}$ as defined below. The signal PDF is proportional to the incoherent sum of the squared matrix elements for different final-state muon helicities ($\lambda_{\mu^+}, \lambda_{\mu^-}$), and depends on the set of fit parameters, $\vec{\omega}$, which includes masses, widths, and helicity couplings of intermediate states contributing to $B^0 \rightarrow J/\psi\phi K_S^0$ decays,

$$\mathcal{P}_{\text{sig}}(m_{\phi K_S^0}^i, \vec{\Omega}^i | \vec{\omega}) = \frac{1}{I(\vec{\omega})} \sum_{\lambda_{\mu^+} \lambda_{\mu^-}} \sum_f |\mathcal{M}_f(m_{\phi K_S^0}^i, \vec{\Omega}^i | \vec{\omega})|^2 \Phi(m_{\phi K_S^0}^i, \vec{\Omega}^i) \epsilon(m_{\phi K_S^0}^i, \vec{\Omega}^i). \quad (2)$$

The term $\Phi(m_{\phi K_S^0}^i, \vec{\Omega}^i)$ represents the phase-space density, the term $\epsilon(m_{\phi K_S^0}^i, \vec{\Omega}^i)$ represents the efficiency, and the term $I(\vec{\omega})$ is a normalisation factor. The efficiency is obtained from simulated samples. Since the $B^0 \rightarrow J/\psi\phi K_S^0$ decay is a self-charge-conjugated mode, the data sample contains both B^0 and \bar{B}^0 decays with unknown b flavour. Therefore, the signal PDF for the neutral B decay averages B^0 and \bar{B}^0 contributions, where the flavour of B candidates is denoted as f in Eq. 2.

The matrix element $\mathcal{M}_f(m_{\phi K_S^0}^i, \vec{\Omega}^i | \vec{\omega})$ is constructed based on the helicity formalism [26]. Three interfering decay sequences are considered: $B^0 \rightarrow (K^* \rightarrow \phi K_S^0) J/\psi$, $B^0 \rightarrow (X \rightarrow J/\psi\phi) K_S^0$, and $B^0 \rightarrow (T_{\psi s1} \rightarrow J/\psi K_S^0) \phi$.⁴ The decay sequences can be described by $m_{\phi K_S^0}$ and $\vec{\Omega} \equiv (\theta_{K^*}, \theta_{J/\psi}, \theta_\phi, \Delta\varphi_{K^* J/\psi}, \Delta\varphi_{K^* \phi})$, where the θ_{K^*} , $\theta_{J/\psi}$, and θ_ϕ are the helicity angles of the ϕ , μ , and K^+ particles in the K^* , J/ψ , and ϕ rest frames, respectively. The angles between the K^* and J/ψ decay planes, and between the K^* and ϕ decay planes in the B rest frame, are denoted as $\Delta\varphi_{K^* J/\psi}$, and $\Delta\varphi_{K^* \phi}$, respectively. The background PDF $\mathcal{P}_{\text{bkg}}(m_{\phi K_S^0}^i, \vec{\Omega}^i)$ is determined from studying the candidates in the sideband of the $m_{J/\psi\phi K_S^0}$ distribution with the methods outlined in Ref. [25].

The default model is taken from Ref. [9] and is composed of nine K^* components, seven X components, and two $T_{\psi s1}$ states ($T_{\psi s1}^\theta(4000)$ and $T_{\psi s1}(4220)$), and one $J/\psi\phi$ nonresonant component (NR). Relativistic Breit–Wigner functions are used to model the lineshapes of these resonances. As shown in Fig. 1, the $B^+ \rightarrow J/\psi\phi K^+$ and $B^0 \rightarrow J/\psi\phi K_S^0$ decays are mediated by the same $b \rightarrow c\bar{c}s$ process and they differ only in the spectator quark, either u or d , which hadronises to the K^+ or K_S^0 meson. The amplitudes of the B^0 and the B^+ decays are formed by intermediate states that are either identical (namely X) or isospin partners (K^* or $T_{\psi s1}$). Under the assumption of isospin symmetry, the mass, width, and helicity couplings for all the components except for the $T_{\psi s1}^\theta(4000)$ states are constrained to be identical. In order to test the significance of the $T_{\psi s1}^\theta(4000)^0$ signal

⁴The K^* denotes any excited K state. The X denotes $\chi_{c0,1}$, η_{c2} , and $T_{\psi\phi 1}^\eta$ states.

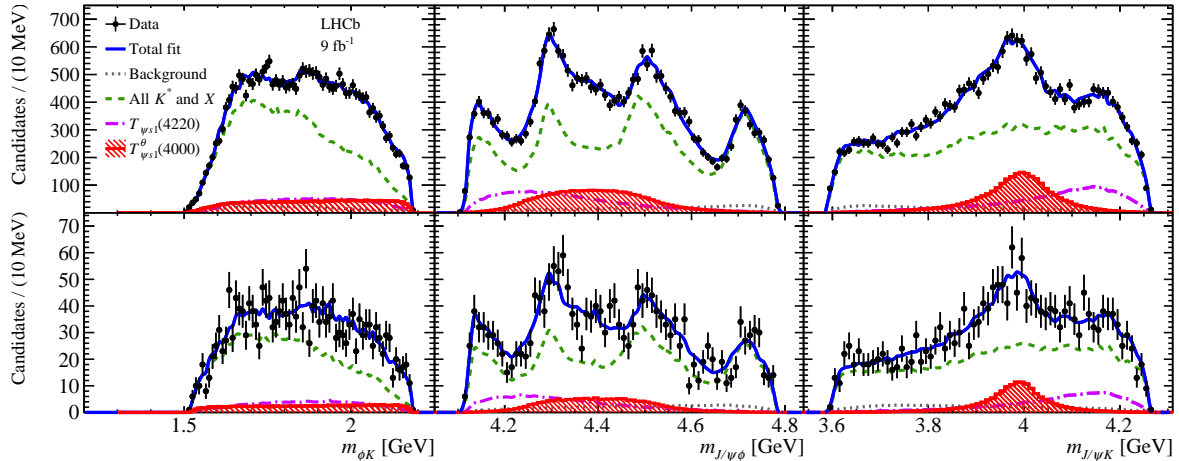


Figure 3: Distributions of (left) $m_{\phi K}$, (middle) $m_{J/\psi\phi}$, and (right) $m_{J/\psi K}$, overlaid with the corresponding projections of the default fit model. The upper and lower rows correspond to the $B^+ \rightarrow J/\psi\phi K^+$ and $B^0 \rightarrow J/\psi\phi K_S^0$ decays, respectively.

Table 1: Results for the $T_{\psi s1}^\theta(4000)^0$ state from the default model. The first uncertainty is statistical and the second systematic.

State	Mass (MeV)	Width (MeV)	Fit fraction (%)	ΔM (MeV)
$T_{\psi s1}^\theta(4000)^0$	$3991^{+12}_{-10} \ ^{+9}_{-17}$	$105^{+29}_{-25} \ ^{+17}_{-23}$	$7.9 \pm 2.5 \ ^{+3.0}_{-2.8}$	$-12^{+11}_{-10} \ ^{+6}_{-4}$

without prior knowledge of its properties, a fit is performed with the masses, widths, and helicity couplings of $T_{\psi s1}^\theta(4000)^0$ and $T_{\psi s1}^\theta(4000)^+$ states allowed to vary independently. In an alternative model, isospin symmetry is imposed for the $T_{\psi s1}^\theta(4000)^0$ and $T_{\psi s1}^\theta(4000)^+$ components. The parameters for the $T_{\psi s1}(4220)^0$ state are always constrained to be identical to the $T_{\psi s1}(4220)^+$ state due to the limited size of the B^0 sample.

Figure 3 shows the ϕK , $J/\psi\phi$, and $J/\psi K$ mass distributions and the corresponding fit projections of the default model for the two B decay modes. Table 1 summarises measurements of the mass, width, fit fraction of the $T_{\psi s1}^\theta(4000)^0$ state, and the mass difference between the $T_{\psi s1}^\theta(4000)^0$ and $T_{\psi s1}^\theta(4000)^+$ states, defined as $\Delta M \equiv M_{T_{\psi s1}^\theta(4000)^0} - M_{T_{\psi s1}^\theta(4000)^+}$. The fit value of ΔM is zero within uncertainties, consistent with the two states being isospin partners. The fit fraction of each component is defined as the integral of the signal PDF divided by the $I(\vec{\omega})$ term. All the fit parameters, including mass, width, and helicity couplings of the intermediate states, of the default model in this analysis are consistent with the corresponding parameters of the default model for the $B^+ \rightarrow J/\psi\phi K^+$ decay in Ref. [9].

The estimated systematic uncertainties on the mass, width, fit fraction of the $T_{\psi s1}^\theta(4000)^0$ state, and on ΔM are summarised in Table 2. Both the background PDF and efficiency function are described by an expansion with Legendre polynomials and a spherical harmonic function instead of interpolation. The effective hadron radius in the Blatt–Weisskopf barrier factor [27], equal to 3 GeV^{-1} in the default model, is replaced with two alternatives, 1.5 and 4.5 GeV^{-1} . The Flatté model [28] including $J/\psi\phi$ and $D_s^{*+}D_s^-$ channels is used for the lineshape of the $X(4140)$ state instead of the relativistic Breit–Wigner model. The representation of the $J/\psi\phi$ NR contribution is changed from a constant

Table 2: Systematic uncertainties associated to the mass, width, fit fraction of the $T_{\psi s1}^\theta(4000)^0$ state, and the mass difference between the $T_{\psi s1}^\theta(4000)^0$ and $T_{\psi s1}^\theta(4000)^+$ states.

Source	Mass (MeV)	Width (MeV)	Fit fraction (%)	ΔM (MeV)
Efficiency and background models	+10.46	+ 1.91	-0.06	+1.02
Hadron radius	+ 0.29 - 1.92	+ 2.33 - 5.85	+0.05 -0.39	+0.92 -1.68
$X(4140)$ Flatté model	+ 0.61	- 3.47	-0.31	-0.18
$J/\psi\phi$ NR representation	+ 1.72	+ 1.46	+0.38	+0.12
Simplified K-Matrix model	- 7.30	-17.54	-1.73	-3.38
Widths of the Breit–Wigner	+ 1.90	- 3.41	-0.56	+1.70
Spin-parity of the $T_{\psi s1}(4220)$ state	-16.32	-17.76	-2.33	-1.48
Non- ϕ contribution	+ 5.52	+ 7.98	+0.92	+5.49
Additional 1^+ $J/\psi\phi$ NR	+ 0.80	- 3.66	+0.18	-1.28
Additional 2^+ $J/\psi\phi$ NR	+ 7.66	+ 2.57	+2.52	+0.92
Extended model	- 6.36	- 2.54	-0.20	-2.98
Additional X state	- 5.58	+ 0.27	+0.34	-1.48
Fit fraction constraint	+ 0.07	+ 1.94	-0.48	-0.45
Impact parameter χ^2 modelling	+ 1.00	- 2.49	-0.22	+0.72
Finite simulation sample size	+ 2.90	+11.20	+1.33	+2.17
Fixed mass and width of K^* states	- 0.58	- 1.30	-0.43	-0.58
Samples to construct the \mathcal{P}_{bkg}	+ 1.06 - 1.38	+ 6.38 - 7.25	+0.54 -0.59	+0.52 -0.68
Background fraction uncertainty	+ 0.37 - 0.45	+ 1.38 - 1.55	+0.06 -0.07	+0.22 -0.38
Final	+ 8.46 -16.71	+17.09 -23.33	+3.00 -2.84	+6.04 -4.23

to a linear function. The K^* states are described by a simplified one-channel K-matrix model [2] instead of a sum of relativistic Breit–Wigner functions. The mass-dependent widths in the relativistic Breit–Wigner function for the K^* resonances are calculated using the decay with the largest branching fraction, $K^* \rightarrow K\pi$ or $K^* \rightarrow K^*(892)\pi$, instead of using the $K^* \rightarrow \phi K$ decay. The spin-parity of the $T_{\psi s1}(4220)$ state is changed from 1^+ to 1^- . The uncertainty originating from the neglected non- ϕ contribution is evaluated by narrowing the ϕ mass window from ± 15 MeV to ± 8 MeV. An additional $J/\psi\phi$ NR contribution with the spin-parity equal to 1^+ or 2^+ is included. An extended model with more K^* states is also studied, which includes all the K^* resonances that are within the allowed phase space, as predicted in Ref. [29]. Possible additional X states, with spins ranging from 0 to 2, are checked in the extended model. The total fit fraction of the default model is 165.2%, which indicates that the interference between the decay amplitudes is large. An alternative fit constraining the total fit fraction to be smaller than 140%, corresponding to a reduction by three times its uncertainty, is performed. The final positive (negative) systematic uncertainty is taken as the maximal positive (negative) deviation from the model uncertainties above summed in quadrature with the uncertainty from other sources. These other sources include mismodelling of the impact parameter χ^2 of B candidates, the finite size of the simulated samples, the fixed masses and widths of the known K^* states, the choice of the data sample used to construct the background PDF model, and the uncertainty on the background fraction.

The significance of the $T_{\psi s1}^\theta(4000)^0$ state is evaluated with a likelihood ratio test.

The test statistic is defined as $t \equiv -2 \ln[\mathcal{L}(H_0)/\mathcal{L}(H_1)]$ with H_1 and H_0 denoting the default model with and without the $T_{\psi_{s1}}^\theta(4000)^0$ state. Here, the term \mathcal{L} represents the likelihood of the B^0 decay. Five thousand pseudoexperiments are generated with the H_0 model, where the parameters of the model are fixed to the values determined from data. The sample size of each pseudoexperiment follows a Poisson distribution with its mean being equal to the number of candidates in the data sample. A fit is performed to each pseudoexperiment with the H_0 and H_1 models to determine the test statistic t . A χ^2 function with the number of degrees-of-freedom allowed to vary is used to fit the t distribution from these pseudoexperiments. Using the resulting χ^2 function, the probability of $t > t_{\text{data}}$ is taken as the p -value. The corresponding significance is estimated to be 4.9σ , decreasing to 4.0σ after including systematic uncertainties, which provides evidence for the $T_{\psi_{s1}}^\theta(4000)^0$ state. The significance for the $T_{\psi_{s1}}^\theta(4000)^0$ state is taken as the smallest significance found when varying the sources of systematic uncertainty.

The significance is also evaluated assuming isospin symmetry for the $T_{\psi_{s1}}^\theta(4000)$ states, where the test statistic is defined as $t' \equiv -2 \ln[\mathcal{L}(H_0)/\mathcal{L}(H'_1)]$ with \mathcal{L} denoting the total likelihood of the B^+ and B^0 decays. The corresponding fit parameters for the $T_{\psi_{s1}}^\theta(4000)^+$ and $T_{\psi_{s1}}^\theta(4000)^0$ states, including mass, width, and helicity couplings, are constrained to be equal between the two states in the H'_1 model. A fit is performed to the t' distribution from the pseudoexperiments with a Gaussian function. The Gaussian function rather than a χ^2 distribution is used here because the number of degree-of-freedom of the H_0 and H'_1 models are equal. The significance is estimated to be 7.2σ and decreases to 5.4σ after accounting for systematic uncertainties.

In conclusion, an amplitude analysis of the $B^0 \rightarrow J/\psi\phi K_S^0$ decay is performed. Evidence of a $J/\psi K_S^0$ structure, denoted the $T_{\psi_{s1}}^\theta(4000)^0$ state, is obtained with a significance of 4.0σ . The mass and width of this state are measured to be

$$\begin{aligned} M(T_{\psi_{s1}}^\theta(4000)^0) &= 3991_{-10}^{+12} {}_{-17}^{+9} \text{ MeV}, \\ \Gamma(T_{\psi_{s1}}^\theta(4000)^0) &= 105_{-25}^{+29} {}_{-23}^{+17} \text{ MeV}, \end{aligned}$$

where the first uncertainty is statistical and the second systematic. The mass difference between the $T_{\psi_{s1}}^\theta(4000)^0$ and $T_{\psi_{s1}}^\theta(4000)^+$ states is measured to be

$$\Delta M = -12_{-10}^{+11} {}_{-4}^{+6} \text{ MeV},$$

which is consistent with the two states being isospin partners. With isospin symmetry imposed for the $T_{\psi_{s1}}^\theta(4000)$ states, the significance of the $T_{\psi_{s1}}^\theta(4000)^0$ structure is measured to be 5.4σ .

References

- [1] Belle collaboration, S. K. Choi *et al.*, *Observation of a narrow charmonium-like state in exclusive $B^\pm \rightarrow K^\pm \pi^+ \pi^- J/\psi$ decays*, Phys. Rev. Lett. **91** (2003) 262001, arXiv:hep-ex/0309032.
- [2] Particle Data Group, R. L. Workman *et al.*, *Review of particle physics*, Prog. Theor. Exp. Phys. **2022** (2022) 083C01.
- [3] LHCb collaboration, R. Aaij *et al.*, *Observation of structure in the J/ψ -pair mass spectrum*, Science Bulletin **65** (2020) 1983, arXiv:2006.16957.
- [4] ATLAS collaboration, *Observation of an excess of di-charmonium events in the four-muon final state with the ATLAS detector*, ATLAS-CONF-2022-040.
- [5] CMS collaboration, *Observation of new structures in the $J/\psi J/\psi$ mass spectrum in pp collisions at $\sqrt{s} = 13$ TeV*, CMS-PAS-BPH-21-003.
- [6] LHCb collaboration, R. Aaij *et al.*, *Observation of a narrow pentaquark state, $P_c(4312)^+$, and of two-peak structure of the $P_c(4450)^+$* , Phys. Rev. Lett. **122** (2019) 222001, arXiv:1904.03947.
- [7] LHCb collaboration, R. Aaij *et al.*, *Observation of a $J/\psi\Lambda$ resonance consistent with a strange pentaquark candidate in $B^- \rightarrow J/\psi\Lambda\bar{p}$ decays*, arXiv:2210.10346, submitted to Phys. Rev. Lett.
- [8] BESIII collaboration, M. Ablikim *et al.*, *Observation of a near-threshold structure in the K^+ recoil-mass spectra in $e^+e^- \rightarrow K^+(D_s^- D^{*0} + D_s^{*-} D^0)$* , Phys. Rev. Lett. **126** (2021) 102001, arXiv:2011.07855.
- [9] LHCb collaboration, R. Aaij *et al.*, *Observation of new resonances decaying to $J/\psi K^+$ and $J/\psi\phi$* , Phys. Rev. Lett. **127** (2021) 082001, arXiv:2103.01803.
- [10] LHCb collaboration, T. Gershon *et al.*, *Exotic hadron naming convention*, arXiv:2206.15233.
- [11] L. Meng, B. Wang, and S.-L. Zhu, *$Z_{cs}(3985)^-$ as the U -spin partner of $Z_c(3900)^-$ and implication of other states in the $SU(3)_F$ symmetry and heavy quark symmetry*, Phys. Rev. **D102** (2020) 111502, arXiv:2011.08656.
- [12] L. Maiani, A. D. Polosa, and V. Riquer, *The new resonances $Z_{cs}(3985)$ and $Z_{cs}(4003)$ (almost) fill two tetraquark nonets of broken $SU(3)_f$* , Science Bulletin **66** (2021) 1616, arXiv:2103.08331.
- [13] BESIII collaboration, M. Ablikim *et al.*, *Evidence for a neutral near-threshold structure in the K_S^0 recoil-mass spectra in $e^+e^- \rightarrow K_S^0 D_s^+ D^{*-}$ and $e^+e^- \rightarrow K_S^0 D_s^{*+} D^-$* , Phys. Rev. Lett. **129** (2022) 112003, arXiv:2204.13703.
- [14] LHCb collaboration, A. A. Alves Jr. *et al.*, *The LHCb detector at the LHC*, JINST **3** (2008) S08005.

- [15] LHCb collaboration, R. Aaij *et al.*, *LHCb detector performance*, Int. J. Mod. Phys. **A30** (2015) 1530022, [arXiv:1412.6352](#).
- [16] T. Sjöstrand, S. Mrenna, and P. Skands, *A brief introduction to PYTHIA 8.1*, Comput. Phys. Commun. **178** (2008) 852, [arXiv:0710.3820](#); T. Sjöstrand, S. Mrenna, and P. Skands, *PYTHIA 6.4 physics and manual*, JHEP **05** (2006) 026, [arXiv:hep-ph/0603175](#).
- [17] D. J. Lange, *The EvtGen particle decay simulation package*, Nucl. Instrum. Meth. **A462** (2001) 152.
- [18] Geant4 collaboration, J. Allison *et al.*, *Geant4 developments and applications*, IEEE Trans. Nucl. Sci. **53** (2006) 270; Geant4 collaboration, S. Agostinelli *et al.*, *Geant4: A simulation toolkit*, Nucl. Instrum. Meth. **A506** (2003) 250.
- [19] M. Clemencic *et al.*, *The LHCb simulation application, Gauss: Design, evolution and experience*, J. Phys. Conf. Ser. **331** (2011) 032023.
- [20] W. D. Hulsbergen, *Decay chain fitting with a Kalman filter*, Nucl. Instrum. Meth. A: **552** (2005) 566.
- [21] W. S. McCulloch and W. Pitts, *A logical calculus of the ideas immanent in nervous activity*, Bull. Math. Biol **5** (1943) 115.
- [22] F. Rosenblatt, *The perceptron: A probabilistic model for information storage and organization in the brain*, Psy. Rev. **65** (1958) 386–408.
- [23] LHCb collaboration, R. Aaij *et al.*, *Amplitude analysis of $B_s^0 \rightarrow K_S^0 K^\pm \pi^\mp$ decays*, JHEP **06** (2019) 114, [arXiv:1902.07955](#).
- [24] D. Martínez Santos and F. Dupertuis, *Mass distributions marginalized over per-event errors*, Nucl. Instrum. Meth. **A764** (2014) 150, [arXiv:1312.5000](#).
- [25] LHCb collaboration, R. Aaij *et al.*, *Amplitude analysis of $B^+ \rightarrow J/\psi \phi K^+$ decays*, Phys. Rev. **D95** (2017) 012002, [arXiv:1606.07898](#).
- [26] S. U. Chung, *Spin formalisms*, CERN-71-08 (1971) ; J. D. Richman, *An experimenter's guide to the helicity formalism*, CALT-68-1148; M. Jacob and G. C. Wick, *On the general theory of collisions for particles with spin*, Annals Phys. **7** (1959) 404.
- [27] J. M. Blatt and V. F. Weisskopf, *Theoretical nuclear physics*, John Wiley and Sons, New York, 1952. p. 361.
- [28] S. M. Flatté, *Coupled-channel analysis of the $\pi\eta$ and $K\bar{K}$ systems near $K\bar{K}$ threshold*, Phys. Lett. **B63** (1976) 224.
- [29] S. Godfrey and N. Isgur, *Mesons in a relativized quark model with chromodynamics*, Phys. Rev. **D32** (1985) 189.